Polymer Testing 113 (2022) 107656

Contents lists available at ScienceDirect

Polymer Testing

journal homepage: www.elsevier.com/locate/polytest

Temperature modulated DSC for composition analysis of recycled polyolefin blends

Andromeda Scoppio [a,b], Dario Cavallo [c,**], Alejandro J. Müller [b,d,*], Davide Tranchida [a,***]

[a] Borealis Polyolefine GmbH, Innovation Headquarters, St. Peterstrasse 25, 4021, Linz, Austria
[b] POLYMAT and Department of Polymers and Advanced Materials: Physics, Chemistry and Technology, Faculty of Chemistry, University of the Basque Country UPV/EHU, Paseo Manuel de Lardizabal, 3, 20018, Donostia-San Sebastián, Spain
[c] Dipartimento di Chimica e Chimica Industriale, Università degli studi di Genova, via Dodecaneso 31, 16146, Genova, Italy
[d] IKERBASQUE, Basque Foundation for Science, Plaza Euskadi 5, 48009, Bilbao, Spain

ARTICLE INFO

Keywords:
Recycled polyolefin blends
TMDSC
Composition analysis

ABSTRACT

Post-consumer plastic waste contains blends of numerous types of polyethylene (PE) and isotactic polypropylene (i-PP), whose recycling is challenging due to the complexity of this waste stream. A comprehensive knowledge of the composition of these recyclates is essential to understand the structure-property relationship of these systems and therefore upcycle them for high-value applications. To this aim, we used Temperature Modulated DSC (TM-DSC) to develop a quantitative method to evaluate PE and Low-density PE (LDPE) content in recycled polyolefin blends. TM-DSC was carried out on 29 virgin PE materials, spanning densities between 960 and 862 kg/m^3, characterizing a wide range of PE microstructures. Moreover, several PE/i-PP model blends were prepared by selecting LDPE, High-density PE (HDPE) and Linear Low-density PE (LLDPE) materials to blend them with i-PP of three types: homopolymer (PP–H), block copolymer (PP–B) and random copolymer (PP-R), mimicking the composition of real recyclates. Results from the TM-DSC analysis of these blends allowed us to establish methods for quantifying the amount of overall PE content and also the LDPE fraction within recyclates. The developed methods were applied to real *post*-consumer recycled grades, and results were compared with the ones obtained from Cross-Fractionation Chromatography (CFC) analysis and Nuclear Magnetic Resonance (NMR) spectroscopy, displaying good agreement between the latter and the TM-DSC method.

1. Introduction

In 2019 plastic production reached 368 Mt globally and 57.9 Mt in Europe, with polyolefins (POs), specifically Polyethylene (PE) and isotactic-Polypropylene (i-PP), as top-demanded polymers in the European plastics market [1]. As a matter of fact, POs are nowadays used for a breadth of applications, primarily for packaging materials, but also for pipes, bottles, household appliances, and automotive components [2–4]. Moreover, since they are characterized by high chemical stability and resistance to degradation [5], concerns exist about their environmental impact at the end of their life cycle, especially regarding accumulation in landfills or in marine litter [6,7].

To this day, mechanical recycling, i.e., reprocessing the waste into secondary raw materials and products via mechanical means, through a series of treatments and preparation steps [8], represents the most well-established technology for large-scale plastic waste treatment, both environmentally and economically [8,9]. For instance, the so-called *post*-industrial plastic waste (PIPW), i.e., material generated by industries, often consists of a clearly identified feedstock, clean and with known composition [10], thus suitable to be mechanically recycled. However, among the challenges linked to mechanical recycling of plastics, a relevant one is represented by feedstock heterogeneity [11]. Specifically, in the case of *post*-consumer plastic waste (PCPW), the extremely complex waste stream containing a mixture of several plastic

* Corresponding author. POLYMAT and Department of Polymers and Advanced Materials: Physics, Chemistry and Technology, Faculty of Chemistry, University of the Basque Country UPV/EHU, Paseo Manuel de Lardizabal, 3, 20018, Donostia-San Sebastián, Spain.
** Corresponding author.
*** Corresponding author.
E-mail addresses: andromeda.scoppio@borealisgroup.com (A. Scoppio), dario.cavallo@unige.it (D. Cavallo), alejandrojesus.muller@ehu.es (A.J. Müller), davide.tranchida@borealisgroup.com (D. Tranchida).

https://doi.org/10.1016/j.polymertesting.2022.107656
Received 26 April 2022; Accepted 31 May 2022
Available online 2 June 2022

products, types, and grades, with additives or residuals, generally leads to a recycled product with lower quality [12–14]. According to several studies, for the majority of European countries the most common polymers found in PCPW are POs such as low-density polyethylene (LDPE), high-density polyethylene (HDPE) and i-PP, followed by other thermoplastics, mainly polystyrene (PS), polyvinylchloride (PVC) and polyethylene terephthalate (PET) [15–18].

Due to their different density, POs can be efficiently separated from PS, PVC, and PET via low-cost techniques such as sink-float separation processes [19]. Nonetheless, components of the PO fraction (e.g., i-PP, LDPE, HDPE) are quite close in density values, and therefore they would need sophisticated, time-consuming, and costly protocols to be separated, such as manual sorting [20], magnetic density separation process [21], and X-ray fluorescence spectroscopy [22]. Thus, a combination of various types of PE, such as HDPE, LDPE, Linear Low-density PE (LLDPE) and i-PP is frequently found in our recycled streams. One major difficulty to upcycle these recycled PO blends is that, despite their many similarities, PE and i-PP are immiscible and incompatible both in molten and in solid-state, exhibiting phase separation when blended together due to their poor interfacial adhesion [23–26].

While blends of virgin HDPE, LLDPE, LDPE with or without i-PP materials have been characterized in their morphology, thermal and mechanical properties by a wide range of analytical techniques [27–29], such knowledge is currently lacking for *post*-consumer recycled POs. Research reported in the literature shows the use of well-known analytical techniques, such as FTIR (Fourier Transform Infra-Red) and NMR (Nuclear Magnetic Resonance) spectroscopies, for composition analysis of blends of recycled POs [30–32], along with a few studies employing traditional fractionation methods, such as Temperature Rising Elution Fractionation (TREF) and Crystallization Analysis Fractionation (CRYSTAF) [33]. Moreover, thermal fractionation techniques such as Successive Self-Nucleation and Annealing (SSA) have been recently applied to recycled PO blends [34].

Despite their ability to differentiate the content of PE into its fractions (LDPE, LLDPE, and HDPE), NMR and fractionation methods often require expensive instrumentations, high competence, and time-consuming measurements. On the contrary, FTIR measurements are easy and quick to perform, allowing quantification of PE and i-PP fractions in the recyclates [30,32], however, the presence of different PE microstructures cannot be assessed, and often spectra cannot be clearly assigned due to the complexity of recyclates [31].

Thermal analysis, and specifically Differential Scanning Calorimetry (DSC), which is already widely used to characterize polyolefins [35–37], represents a suitable candidate for composition analysis of recyclates. As a matter of fact, its application to the analysis of mixed plastic waste and recycled PO blends is extensively reported in the literature, both for quantitative and qualitative purposes [30–32,38,39]. The basic principle of DSC analysis is the differentiation of the various components based on their different thermal behaviour, and blends of POs were found to have relatively clear and differentiated crystallization and melting of the PE and i-PP fractions, thus allowing their quantification also in the recycled grades. PE and i-PP are indeed characterized by significantly different melting temperatures [25], used for identification of the polymers, while the estimation of their content is usually carried out using the melting enthalpy of both components to establish calibration curves. For instance, Manivannan et al. [39] prepared HDPE/i-PP blends with different compositions and they analyzed them with DSC, establishing a linear trend between the measured enthalpy of fusion of PE and i-PP and their respective content in the blends. This correlation was then used as a calibration curve to determine the contents of PE and i-PP in a *post*-consumer waste plastics sample. According to the authors, results were consistent with the ones from X-ray diffraction. More recently, the same principle was employed by Larsen et al. [30] to quantify the PE fraction in recycled i-PP samples collected from different *post*-consumer waste streams. A procedure was developed to separately estimate the melting enthalpy for PE and i-PP, since they found a partial overlap of the PE and i-PP melting peaks. Therefore, the corrected enthalpy of fusion of PE was calculated and correlated with its content for each PE/i-PP blend produced, displaying linear trends albeit different results depending on the type of PE used in those blends.

Nevertheless, it is known that the PE fraction within recycled grades often contains different types of PE, such as LDPE, LLDPE, and HDPE, whose melting occurs over the same temperature range, resulting in an overlap of their peaks [27,40]. Thus, in the case of recycled PO blends, one cannot differentiate and quantify each PE component based on standard DSC measurements alone.

Within this context, Temperature-Modulated DSC (TM-DSC), a DSC mode in which a periodical temperature modulation is applied over a traditional linear heating/cooling ramp [41], represents a powerful tool for characterization of these types of blends, since it provides more information than the conventional DSC regarding the thermal behaviour of different PE microstructures [42].

The technique, developed by Reading and co-workers in 1992 and patented by TA instruments [43], has reported advantages with respect to standard DSC, including better resolution and sensitivity, along with the ability to separate overlapping thermal phenomena [44]. According to the approach proposed by Reading [44] and then used by Wunderlich et al. [45], a sinusoidal temperature modulation is used, and a mathematical procedure (e.g., discrete Fourier Transform) is applied to deconvolute the calorimetric response to the perturbation from the one to the underlying (i.e., linear) temperature profile. In this way, it is possible to separate the total heat flow (sum of all thermal events occurring in the sample at the considered temperature range) into two different components, as shown below in Equation (1):

$$dQ \,/\, dt = C_p b + f(T,t) \tag{1}$$

where dQ/dt is the resultant heat flow into the sample, C_p represents the heat capacity of the sample due to its molecular motions, $b = dT/dt$ the heating rate, and $f(T,t)$ is the heat flow arising from kinetic events. Specifically, in TM-DSC, the heat capacity component ($C_p b$) is referred to as Reversing Heat Flow (R–HF), while the kinetic component $f(T,t)$ as Non-Reversing Heat Flow (NR-HF), where the terms “reversing” and “non-reversing” are here used to describe processes that are either reversible or irreversible at the time and temperature at which the measurement is made [41,46]. Since the reversing component is related to the sample’s heat capacity, while the non-reversing one reflects only irreversible phenomena, the ability of TM-DSC of splitting the heat flow into these components is particularly interesting and useful when applied to processes like polymer melting, whose nature is mostly thermodynamically reversible but also contains a non-reversing character due to exothermic phenomena such as recrystallization, crystal annealing and perfection of non-equilibrium crystals [47,48]. These phenomena can be resolved in the NR-HF, thus allowing the separation of crystallization exotherms from heat capacity related events, such as glass transition and reversible melting.

As thoroughly reported in the work of Wunderlich [49], TM-DSC has been used for the characterization of the melting and crystallization behaviour of several polymers, although it has been exploited mainly to investigate the reversible melting process. Specifically, various studies done by Cser et al. [50–52], illustrate how semicrystalline polymers always display some reversibility in melting, whose extent is a function of the modulation frequency, amplitude, and chemical structure of the polymer.

PEs are the most widely tested materials with TM-DSC [42,51,53–56]. For instance, within these works, one in particular, showed the application of TM-DSC to LLDPE/i-PP blends prepared with and without poly(styrene-*b*-butadiene-*b*-styrene) (SEBS) as compatibilizing agent [51]. The non-reversing enthalpy, in particular, displayed a correlation with the LLDPE content of the blends, however, no explanations about how the NR-HF traces were integrated were provided.

Moreover, Amarasinghe et al. [53] studied the melting behaviour of

different commercial PEs with the TM-DSC. Samples of PE with densities between 908 kg/m^3 and 953 kg/m^3, such as Very Low-density Polyethylene (VLDPE), LDPE, LLDPE, and HDPE, were subjected to different thermal treatments (e.g., slow cooling, fast cooling) and analyzed with the TM-DSC. Specifically, sharp endothermic peaks were found in most of the NR-HF traces of HDPE samples, while highly branched LDPE, LLDPE, and VLDPE samples showed broad exotherms during heating. This phenomenon was likely linked to structural heterogeneity, which led to the formation of thermally unstable thin lamellar crystals.

Eventually, numerous PE materials with density between 918 and 960 kg/m^3 were characterized with TM-DSC by Chau et al. [42] under different experimental conditions. Both reversing and non-reversing heat flows were evaluated, which showed the link between the results and test parameters such as heating rate and modulation period. In detail, three exothermic contributions were identified in the NR-HF traces of an LLDPE sample with a density of 920 kg/m^3 and C8 co-monomer, where these species were well detectable for modulation period up to 60 s and heating rate of 2 °C/min. Moreover, the effects of the molecular architecture of the materials on the NR-HF curves was also studied. Similar to results reported by others [53,57], only endothermic contributions were found in NR-HF traces of HDPE samples, while broad exotherms characterized the NR-HF curves of PE with microstructural heterogeneity, such as LDPE and LLDPE.

In this work, TM-DSC has been used to develop quantitative methods for evaluating the composition of recycled PO blends, with the aim of identifying the type and amount of the PE fraction and quantifying the LDPE component within the latter. Eventually, the methods developed with the TM-DSC were applied to two types of real recycled grades, and the results obtained were then compared with the ones from well-established analytical techniques, specifically Cross-Fractionation Chromatography (CFC) analysis and Nuclear Magnetic Resonance (NMR) spectroscopy.

2. Experimental

2.1. Materials

All the materials studied and investigated in this work were kindly supplied by Borealis GmbH. To perform the TM-DSC analysis over a broad range of PE microstructures, several commercial virgin PE grades were tested in the first part of this work, for a total of 29 virgin PE materials analyzed. These grades belong to the following PE classes: High Density Polyethylene (HDPE), Ziegler-Natta Linear Low-density Polyethylene (ZN-LLDPE), Plastomer (octene-1 as comonomer), metallocene Linear Low-Density Polyethylene (m-LLDPE), and Low-Density Polyethylene (LDPE), the latter obtained with two different technologies: tubular or autoclave reactors. Table 1 lists all the virgin PE grades studied, along with their densities and Melt Flow Rates (MFR). The name assigned to each grade indicates the PE type (HDPE, LDPE, etc.) and density, with the addition of the MFR in case of more than one grade with the same density. Moreover, for LLDPE grades, the catalyst is also indicated by the prefix (ZN) and (m) for Ziegler-Natta and metallocene, respectively. In the case of LDPE samples, the prefixes (T) and (A) stand for tubular and autoclave technology. For instance, (T)LDPE-923_0.75 (T) indicates a virgin LDPE obtained via tubular technology, with a density of 923 kg/m^3 and MFR equal to 0.75 g/10 min.

Furthermore, some of the HDPE, LLDPE, and LDPE grades listed in Table 1 were blended with three different types of isotactic PP: i-PP homopolymer (PP–H), i-PP block copolymer (PP–B), and i-PP random copolymer (PP-R), in different concentrations to mimic the composition of real recycled polyolefin blends, and these will be referred to as "model PO blends". For their preparation, the single components were mixed in a HAAKE™ kneader for 10 min at a screw speed of 50 rpm, and then the resulting product was milled to reduce its size. Eventually, 24 different model PO blends were prepared, that can be sorted by 5 series: LDPE/HDPE/PP-H, LDPE/LLDPE/PP-H, LDPE/HDPE/PP-B, LDPE/HDPE, and LDPE/HDPE/PP-H/PP-R. Table 2 contains the specifics of each blend prepared, including its series, name, types, and amounts of virgin grades used. The name assigned to each model blend contains the acronyms of

Table 1
List of virgin PE grades employed sorted by density (from high to low), along with the grade type and Melt Flow Rate values (MFR_2 = 190 °C/2.16 kg, MFR_5 = 190 °C/5.0 kg, MFR_{21} = 190 °C/21.0 kg).

Name	Type	Density [Kg/m^3]	MFR_2 [g/10 min]	MFR_5 [g/10 min]	MFR_{21} [g/10 min]
HDPE-960	HDPE	960	0.7	_	42
HDPE-954-4	HDPE	954	4	_	_
HDPE-954_0.3	HDPE	954	0.3	1.5	32
HDPE-952_<1	HDPE	952	<1	0.25	7
HDPE-952	HDPE	952	_	_	2.5
HDPE-948	HDPE	948	_	0.8	_
HDPE-946	HDPE	946	<0.1	0.2	6
HDPE-945	HDPE	945	0.3	1.1	25
HDPE-937	HDPE	937	_	5	42
HDPE-937_0.4	HDPE	937	0.4	2.1	42
HDPE-935	HDPE	935	_	0.6	15
HDPE-931	HDPE	931	_	0.9	20
(ZN)LLDPE-931	Ziegler-Natta LLDPE	931	0.2	0.9	20
(ZN)LLDPE-923_0.2	Ziegler-Natta LLDPE	923	0.2	1	22
(ZN)LLDPE-923_0.4	Ziegler-Natta LLDPE	923	0.4	_	_
(T)LDPE-923_0.75	LDPE (Tubular technology)	923	0.75	_	_
(T)LDPE-923_4	LDPE (Tubular technology)	923	4	_	_
(T)LDPE-923_2	LDPE (Tubular technology)	923	2	_	_
(T)LDPE-923_2*	LDPE (Tubular technology) *with additives	923	2	_	_
(T)LDPE-923_0.75	LDPE (Tubular technology)	923	0.75	_	_
(A)LDPE-922_2.1	LDPE (Autoclave technology)	922	2.1	_	_
(A)LDPE-922_1.2	LDPE (Autoclave technology)	922	1.2	_	_
(T)LDPE-920	LDPE (Tubular technology)	920	0.25	_	_
(A)LDPE-920	LDPE (Autoclave technology)	920	0.25	_	_
(m)LLDPE-918	Metallocene LLDPE	918	1.5	_	_
(T)LDPE-918	LDPE (Tubular technology)	918	5	_	_
Plast-902	Ethylene-based octene-1 Plastomer	902	1.1	_	_
Plast-882	Ethylene-based octene-1 Plastomer	882	1.1	_	_
Plast-862	Ethylene-based octene-1 Plastomer	862	1.1	_	_

Table 2
List of model PO blends prepared, categorized in 5 Series (LDPE/LLDPE/PP-H, LDPE/HDPE/PP-H, LDPE/HDPE/PP-B, LDPE/HDPE and LDPE/HDPE/PP-H/PP-R), along with their name, composition and types of virgin grades used.

Series	Blend name	Composition	PE_1	PE_2	i-PP
LDPE/ LLDPE/ PP-H	**(T)LDPE-920/ (ZN)LLDPE-923_0.4/PP-H_a**	5/45/50	(T) LDPE-920	(ZN) LLDPE-923_0.4	PP-H
	(T)LDPE-920/ (ZN)LLDPE-923_0.4/PP-H_b	10/40/50	(T) LDPE-920	(ZN) LLDPE-923_0.4	PP-H
	(T)LDPE-920/ (ZN)LLDPE-923_0.4/PP-H_c	20/30/50	(T) LDPE-920	(ZN) LLDPE-923_0.4	PP-H
LDPE/ HDPE/ PP-H	**(T)LDPE-923_2/HDPE-946/PP-H_a**	5/45/50	(T) LDPE-923_2	HDPE-946	PP-H
	(T)LDPE-923_2/HDPE-946/PP-H_b	10/40/50	(T) LDPE-923_2	HDPE-946	PP-H
	(T)LDPE-923_2/HDPE-946/PP-H_c	15/35/50	(T) LDPE-923_2	HDPE-946	PP-H
	(T)LDPE-923_2/HDPE-946/PP-H_d	20/30/50	(T) LDPE-923_2	HDPE-946	PP-H
	(T)LDPE-920/ HDPE-946/ PP-H_a	5/45/50	(T) LDPE-920	HDPE-946	PP-H
	(T)LDPE-920/ HDPE-946/ PP-H_b	10/40/50	(T) LDPE-920	HDPE-946	PP-H
	(T)LDPE-920/ HDPE-946/ PP-H_c	20/30/50	(T) LDPE-920	HDPE-946	PP-H
	(T)LDPE-920/ HDPE-937_0.4/PP-H_a	5/25/70	(T) LDPE-920	HDPE-937_0.4	PP-H
	(T)LDPE-920/ HDPE-937_0.4/PP-H_b	10/20/70	(T) LDPE-920	HDPE-937_0.4	PP-H
	(T)LDPE-920/ HDPE-937_0.4/PP-H_c	20/10/70	(T) LDPE-920	HDPE-937_0.4	PP-H
LDPE/ HDPE/ PP-B	**(T)LDPE-923_2/HDPE-946/PP-B_a**	5/45/50	(T) LDPE-923_2	HDPE-946	PP-B
	(T)LDPE-923_2/HDPE-946/PP-B_b	10/40/50	(T) LDPE-923_2	HDPE-946	PP-B
	(T)LDPE-923_2/HDPE-946/PP-B_c	15/35/50	(T) LDPE-923_2	HDPE-946	PP-B
	(T)LDPE-923_2/HDPE-946/PP-B_d	20/30/50	(T) LDPE-923_2	HDPE-946	PP-B
LDPE/ HDPE	**(T)LDPE-923_2/HDPE-935_a**	10/90	(T) LDPE-923_2	HDPE-935	_
	(T)LDPE-923_2/HDPE-935_b	25/75	(T) LDPE-923_2	HDPE-935	_
	(T)LDPE-923_2/HDPE-935_c	50/50	(T) LDPE-923_2	HDPE-935	_
	(T)LDPE-923_2/HDPE-935_d	75/25	(T) LDPE-923_2	HDPE-935	_
LDPE/ HDPE/ PP-H/ PP-R	**(T)LDPE-920/ HDPE-935/ PP-H/PP-R_a**	5/45/40/10	(T) LDPE-920	HDPE-935	PP-H+PP-R
	(T)LDPE-920/ HDPE-935/ PP-H/PP-R_b	10/40/40/ 10	(T) LDPE-920	HDPE-935	PP-H+PP-R
	(T)LDPE-920/ HDPE-935/ PP-H/PP-R_c	15/35/40/ 10	(T) LDPE-920	HDPE-935	PP-H+PP-R

the virgin materials used and letters "a, b, c, d" indicating the respective amounts. For example, the model blend (T)LDPE-920/(ZN)LLDPE-923_0.4/PP-H_a, belonging to the series LDPE/LLDPE/PP-H, contains 5% of (T)LDPE-920 and 45% of (ZN)LLDPE-923_04 PE grades, along with 50% of i-PP Homopolymer (PP–H).

Eventually, two recycled grades from *post*-consumer feedstocks streams, previously analyzed in Borealis with CFC analysis and NMR spectroscopy, were employed in the study to test the TM-DSC methods developed to compare the results obtained with the different analytical techniques. To prevent possible issues with reproducibility of the effectively inhomogeneous materials, the pellets were first homogenized in a X-plore Microcompounder MC15 HT at 190 °C with 50 rpm and then samples were measured 9 times by TM-DSC.

2.2. TM-DSC measurements

For the sample preparation, pellets of each material were pressed into a mould at 190 °C to form plaques, then cut in round samples of ca. 3 mg to be placed in the DSC pan.

All the experiments were run with a TA Instruments Q2000 DSC calibrated with Indium, Zinc, and Tin and operating under 50 mL/min of nitrogen flow. The analysis was carried out using the following thermal history: standard DSC (first heating, cooling, second heating, second cooling all performed at 10 °C/min from −30 °C up to 225 °C) followed by a modulated step, with 2 °C/min heating rate, modulation amplitude ±0.32 °C and modulation period 60 s.

3. Results and discussion

The second heating scans of standard DSC measurements of selected virgin PE grades employed in this study are shown in Fig. 1 for three different sets of materials: HDPE, LLDPE, and LDPE grades. Results indicate how, heating up the samples at 10 °C/min after a first heating and subsequent cooling cycle, the different types of PE grades melt in separate temperature ranges, depending on their microstructures.

In the case of HDPE grades (set of materials at the top of Fig. 1), characterized by little or no chain branching, the structure is highly crystalline, and thus the endothermic peak is quite narrow, in the range of temperatures 110–132 °C. On the contrary, LDPE samples (set of materials at the bottom of Fig. 1), having a complex long-branched structure, display broad endotherms and lower peak melting temperatures at ca. 110 °C. Finally, samples classified as LLDPE, containing α-olefin comonomers, melt at temperatures around ca. 121 °C. Specifically, (ZN)LLDPE-923_0.4 (light blue curve) melts at a slightly higher temperature than (m)LLDPE-918 (green curve). Both materials are obtained from the Borstar® polymerization process, but are characterized by different co-monomer distributions, due to the different number of available active sites in the respective catalyst [58]. (ZN)LLDPE presents a more uneven co-monomer distribution, while in (m)LLDPE there is a homogeneous distribution of defects and therefore shorter crystallizable linear sequences than (ZN)LLDPE [59].

The different melting points found for the PE types (i.e., HDPE, LLDPE, and LDPE) analyzed with the DSC, can be explained by the well-known Gibbs-Thomson equation [60], which correlates the melting point to the lamellar thickness of the polymer crystals:

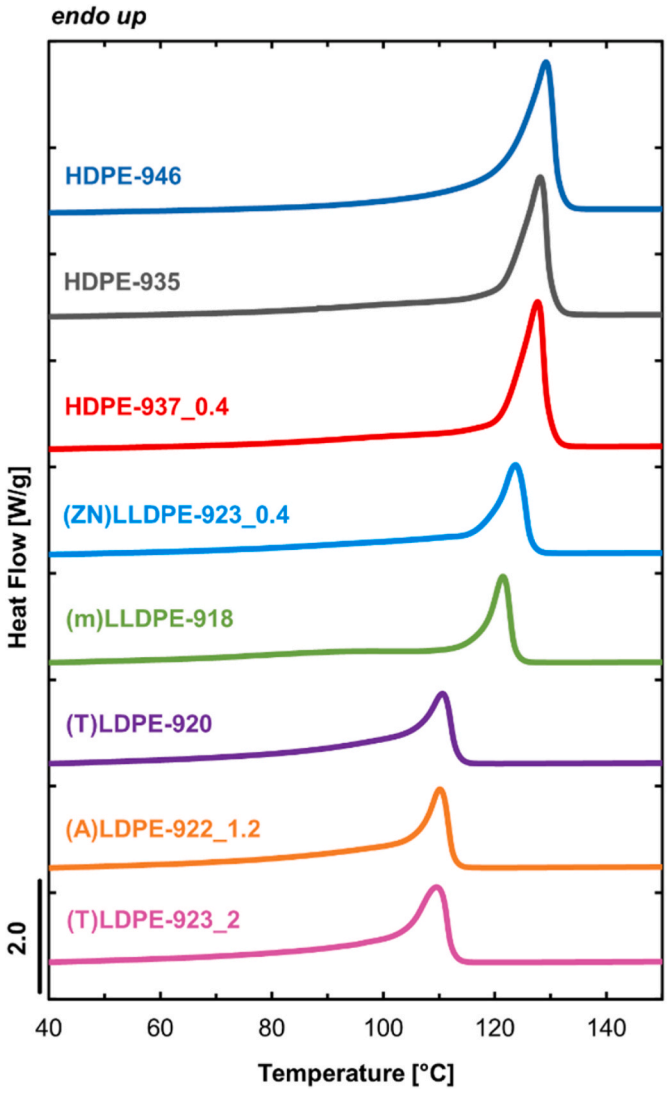

Fig. 1. DSC second heating scans of selected virgin PE grades studied. PE types from top to bottom: HDPE, LLDPE, and LDPE.

$$T_m = T_m^0\left(1 - \frac{2\sigma_e}{\Delta H_m l}\right) \tag{2}$$

where in equation (2) T_m is the observed melting temperature, T_m^0 is the equilibrium melting point of an infinitely thick PE crystal, σ_e is the surface free energy of the basal plane, ΔH_m is the enthalpy of fusion per unit volume, and l is the average thickness of the *lamellae* corresponding to the observed melting temperature. Hence, as seen in Fig. 1, virgin PE grades characterized by high structural regularity (e.g., HDPE), which crystallize in thick *lamellae*, have higher melting points than the ones that have thinner lamellae (e.g., LDPE) [61,62]. As a matter of fact, by correlating the melting temperatures of each grade analyzed with its own density, the trend in Fig. 2 was found, showing an increase of the melting temperature as the density of the grades increases.

Considering the materials with melting temperatures above 120 °C, as it is possible to appreciate in the inset of Fig. 2, one can notice that samples with densities between 918 and 960 kg/m^3, show a linear trend between their density and the measured melting point. Therefore, as will be discussed below, this linear correlation can be used as a calibration curve to predict the density of the PE fraction and thus identifying unequivocally PE types with densities between 918 and 960 kg/m^3 within recycled grades. This is relevant, since, in the case of PE, the density is the key industrial parameter to identify the polymer type (i.e., HDPE, LDPE, LLDPE), and in recycled PO blends a direct measurement of PE density is not experimentally possible.

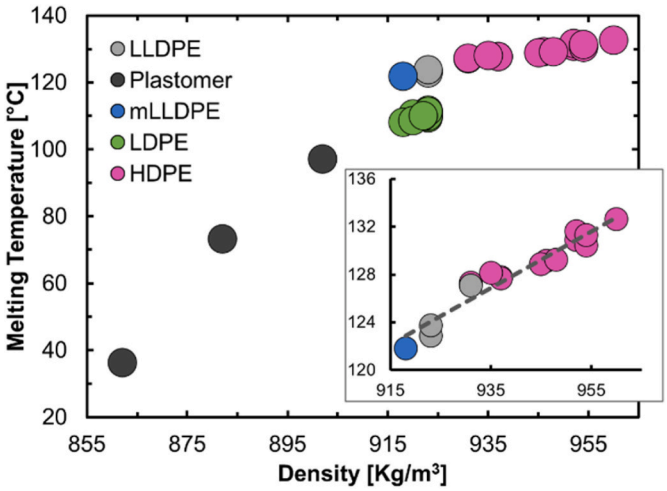

Fig. 2. Peak melting temperature (°C) as a function of density (Kg/m^3) for all the virgin PE grades analyzed with standard DSC. Set of materials: Plastomer (dark grey), LDPE (green), (m)LLDPE (blue), (ZN)LLDPE (light grey) and HDPE (pink). (For interpretation of the references to colour in this figure legend, the reader is referred to the Web version of this article.)

Furthermore, since TM-DSC allows separation of simultaneous thermal phenomena, such as melting, recrystallization, and annealing, by using a periodical temperature modulation superimposed on a linear heating/cooling ramp, the NR-HF curves were used in this work to gain new insights on how the molecular architecture of the resin affects its thermal behavior, indicating the presence of crystal perfection phenomena during the heating process. Fig. 3 contains the non-reversing heat flow (NR-HF) traces of the same set of PEs shown in Fig. 1, from top to bottom: HDPE, LLDPE, and LDPE grades. For the sake of completeness, the Reversing Heat flow traces can be found in Fig. S1 of the Supporting Information (SI).

Specifically, in the case of HDPE samples at the top of Fig. 3, the NR-HF shows only one endotherm with a peak at ca. 128 °C, as the crystallization under cooling at 10 °C/min gives rise to a structure which does not undergo reorganization during the subsequent modulated heating.

A very different thermal behavior was instead found for the LDPE grades at the bottom of Fig. 3, that appear well differentiated from the other PE materials since they show broad exothermic peaks centered at temperatures around 110 °C. These results are reasonable since LDPE molecules have a complex and mixed branched structure, that affects their crystallization during the cooling step of the DSC experiment, thus leading to a broad distribution of lamellar thickness [63]. The fact that virgin HDPE and LDPE samples show a significantly different thermal behaviour in the modulated heating and more specifically in the NR-HF, makes TM-DSC particularly promising for distinguishing the LDPE and HDPE fractions in the recyclates.

Interestingly, TM-DSC analysis of the two LLDPE grades, (ZN)LLDPE-923_0.4 (light blue curve, Fig. 3) and (m)LLDPE-918 (green curve, Fig. 3), shows significantly different thermal behaviors in the NR-HF. Specifically, (ZN)LLDPE-923_0.4 displays a small endothermic peak, while (m)LLDPE-918 shows a broad exotherm. m-LLDPE is characterized by short crystallizable sequences due to the even distribution of chain branching, which are not able to crystallize properly during cooling and therefore experience recrystallization and/or annealing throughout the modulated heating process. ZN-LLDPE, on the other hand, is known to exhibit two types of *lamellae:* thick and long (like the ones of HDPE) and short and curved (due to the presence of branches) [64], therefore, it is characterized by the coexistence of some long

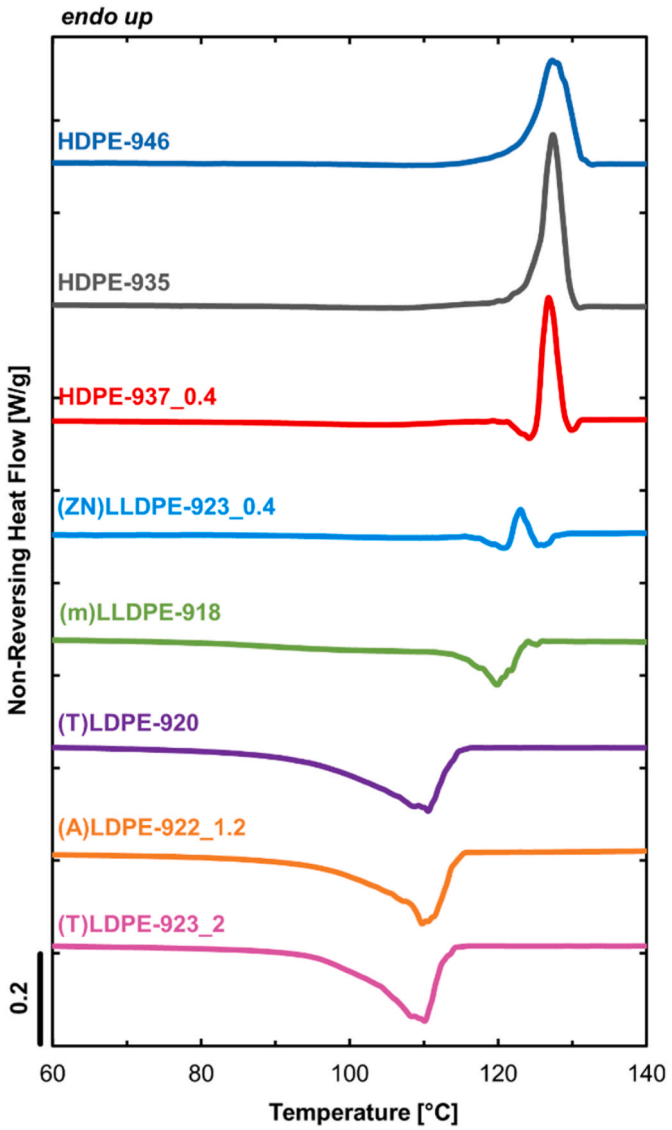

Fig. 3. TM-DSC non-reversing heat flow traces of selected virgin PE grades studied. PE types from top to bottom: HDPE, LLDPE, and LDPE.

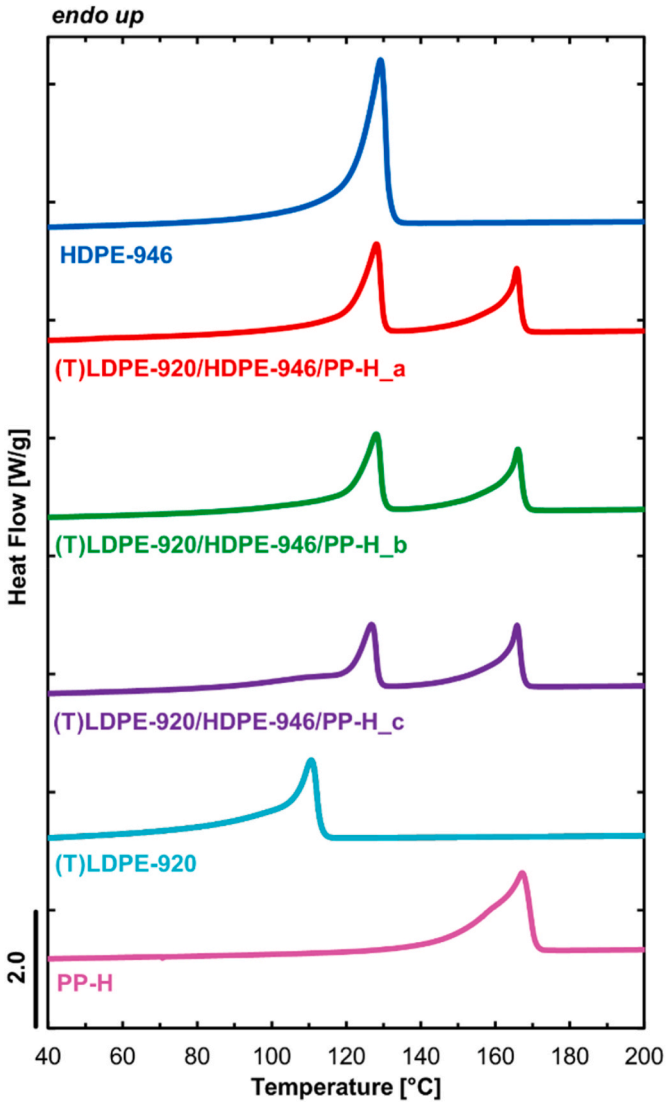

Fig. 4. DSC second heating scans of three different compositions of the model PO blend (T)LDPE-920/HDPE-946/PP-H (a= 5/45/50, b = 10/40/50 and c = 20/30/50) along with the ones of the neat components used: HDPE-946, (T) LDPE-920 and PP-H.

crystallizable sequence lengths that give rise to an endothermic contribution, and short ones that show exothermic phenomena in the NR-HF. This difference between m-LLDPE and ZN-LDPE evaluated in the NR-HF, is also in agreement with the higher melting point of ZN-LLDPE found in the second heating scan of the standard DSC analysis of these samples, as shown in Fig. 1. Again, these findings confirm the ability of TM-DSC to detect differences in the microstructure not possible to be appreciated or identified clearly in a standard DSC measurement.

In Fig. 4, the DSC second heating scans of the model PO blend (T) LDPE-920/HDPE-946/PP-H with different compositions (a = 5/45/50, b = 10/40/50 and c = 20/30/50), can be observed along with the scans of the neat components: (T)LDPE-920 (light blue curve), HDPE-946 (blue curve) and PP-H (bottom pink curve). By looking at the scans of the model blends, one can observe two well distinguished endothermic peaks: one centered at ca. 166 °C, due to melting of the PP-H component, and one at lower temperatures (ca. 128 °C), which can be attributed to the HDPE fraction of the model blend. However, one can notice that the tail of the i-PP component peak is partially superimposed with the melting of the PE phase, as also found in other studies [30,34].

On the other hand, within the PE fraction, the two LDPE and HDPE components appear to be completely overlapped in one melting endotherm, with the exception of the model blend (T)LDPE-920/HDPE-946/PP-H_c (purple curve of Fig. 4), where a main endothermic peak and a lower melting shoulder can be observed below 130 °C. This shoulder at ca. 110 °C, that can be better appreciated in Fig. S2 of SI, presumably belongs to the LDPE contribution to the PE fraction, being in the melting range of the neat (T)LDPE-920 grade (light blue curve in Fig. 4). This shoulder was not detected for the other blend compositions, probably because of their very low LDPE content, i.e., <10 wt%. Moreover, no significant shift of the melting peak temperature occurs for the PP-H grade when mixed in the blends, suggesting relatively weak interactions with the PE components and immiscibility, as also evaluated in other studies concerning thermal properties of these types of blends [65]. Instead, a slight decrease of the melting temperature of the HDPE component can be observed when it is blended with LDPE, that goes from ca. 129 °C (neat HDPE-946) to ca. 127 °C in the model blend (T)LDPE-920/HDPE-946/PP-H_c (purple curve of Fig. 4), where this might indicate some interaction between the two, although not fully explainable by standard DSC scans only [66].

The second heating scan of the standard DSC measurements performed on the model PO blends, was studied and used in this work for

quantifying the PE fraction present in these blends. To this aim, two different methods were employed to determine the amount of PE in the model blends prepared in the study. In the first one, the area under the melting peak of PE (i.e., the enthalpy of fusion) was correlated to the amount of PE in the model blends, to prepare a calibration curve to be used for quantifying the PE fraction in the recycled blends.

Specifically, a linear integration of the second heating scan was carried out between 30 °C and 175 °C, with a vertical drop at 132 °C, as shown in Fig. 5, since it is likely that no PE *lamellae* would melt after this temperature. Nevertheless, as displayed in Fig. 4, the tail of the i-PP melting in these low temperature ranges partially overlaps with the PE phase, whose enthalpy of fusion, therefore, contains a contribution from the i-PP melting enthalpy. The use of DSC analysis on PE/i-PP blends for determining the PE content, by deriving calibration curves, have been reported earlier in the literature [32,67], with studies that focused mainly on few HDPE, LDPE, and i-PP grades, not considering the variety of types, grades, microstructures of PE and i-PP actually present in the recycled blends.

Thus, the described experimental procedure was applied to the model PO blends in Table 2, and results are displayed in Fig. 6. At a first glance, one can notice that there is a significant variability in the melting enthalpy measured for the blends having the same PE amount (30 wt%, 50 wt%, and 100 wt%). For instance, melting enthalpies of 99.4 J/g and 61.2 J/g were recorded for two model blends containing both 50 wt% of PE. This significant difference is, in this case, likely due to the presence of (ZN)LLDPE-923_0.4 in the blends, for which lower enthalpies were measured since this material is less crystalline than the HDPE present in the other blends. Therefore, results from Fig. 6 prove the limits of this approach of calibration curves for determining the PE fraction in the recycled grades since the variability in the melting enthalpy obtained becomes significantly high once different PE and PP types are used in the blends. In the case of real recycled materials, the complexity is even higher than these model blends, and therefore we suggest that the calibration curves approach should not be used.

Given the results obtained with the first procedure, which showed how the melting enthalpy calculation is not reliable to determine the PE amount in the recyclates, an alternative method has been developed. The latter is based on a statistical evaluation of the low-temperature tail of DSC traces of i-PP during melting, performed over 5000 different types of i-PP materials, that led to the development of an actual database of the melting behavior of the i-PP fraction. It was found that homopolymers of i-PP show a relatively constant fraction of melting enthalpy up to 132 °C, which amounts to 11.8 ± 2.5% of the total enthalpy.

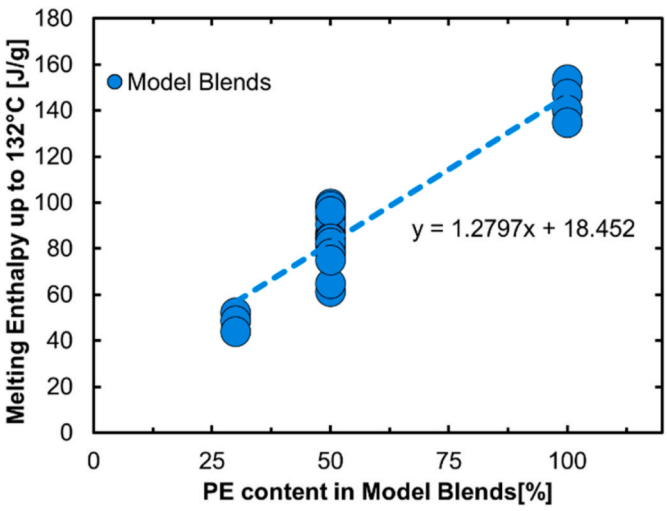

Fig. 6. Melting Enthalpy of DSC second heating scan as a function of the PE content present in the model PO blends prepared in this work.

Therefore, we calculate the melting enthalpy of the blend from 132 °C to the end of the melting, and afterwards calculate the tail towards lower temperatures. This is subtracted from the melting enthalpy up to 132 °C, thus evaluating the melting enthalpy of the PE fraction alone. A similar procedure was reported by Larsen et al. [30], with the difference that in that work, it is suggested to extrapolate the melting curve of the i-PP fraction linearly, which could introduce additional variability and is not soundly justified.

As shown above, the melting temperature of PE can be correlated to the density and equivalently to the melting enthalpy, as shown in the SI (Fig. S3). Therefore, from the value of the melting temperature, we estimate the value of the melting enthalpy for the PE fraction in the blend. Then, the ratio of the measured enthalpy after the i-PP correction and the estimated melting enthalpy for a 100% PE material, provides the PE content in the blend.

Fig. 7 displays the results obtained from the application of the DSC method to the model PO blends prepared in this work, showing a comparison of these results with the actual PE amount present in the blends. As it is possible to observe in Fig. 7, there is a significant agreement between the two PE contents, and although there is some scattering of the points belonging to blends with 50 wt% of PE, this is not as significant as in the case of the first procedure. Specifically, for 50 wt

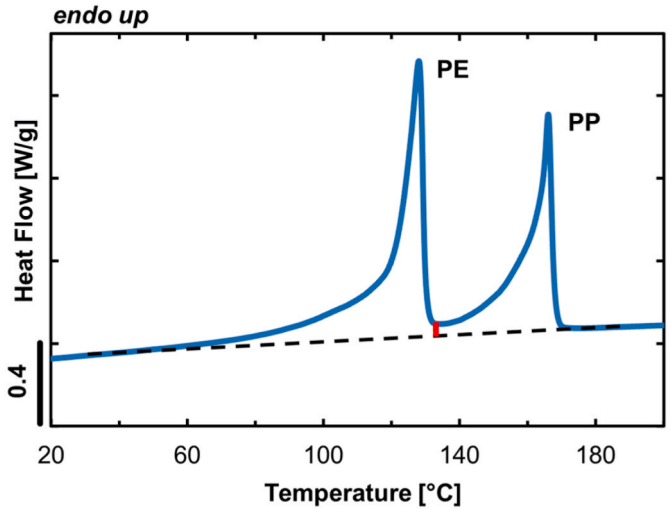

Fig. 5. Schematic of the linear integration of the DSC second heating scan for one of the model blends prepared.

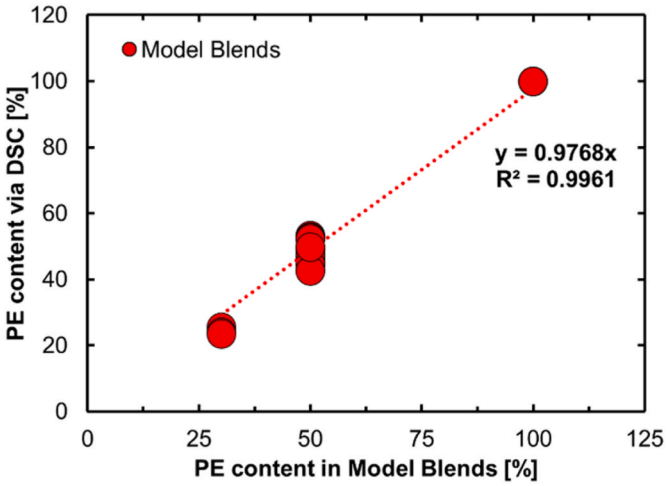

Fig. 7. PE content obtained via DSC as a function of the actual PE content present in the model blends.

% PE, the PE contents obtained from the database method vary from 42.6 wt% to 53.3 wt%, indicating a definitely lower variability in the results with respect to the ones obtained in Fig. 6.

Thus, according to these results, the DSC method is promising for quantifying the PE fraction within the recyclates.

Besides the evaluation of PE content, the DSC second heating scan of the model PO blends prepared was also used to identify the PE type within the recyclates, via the correlation between PE melting peak temperatures and density found for virgin grades with density in the range 918–960 kg/m^3, as already introduced in Fig. 2. Therefore, the peak melting temperatures of the PE fraction of all model PO blends prepared were collected from the DSC second heating scans and then correlated to the density of the PE fraction within each blend. In detail, since it is not possible to directly measure the density of the PE phase dispersed in the i-PP matrix, the density of the PE fraction was estimated as a weighted average of the densities of the single PE components of the blends. This approach is reasonable since physical properties as the density were proved to follow the law of mixture (LOM), and have been used to predict properties of PO blends with known composition and grades [68,69].

Results of this correlation for the model blends are shown in Fig. 8 as green diamonds, along with the ones obtained from the virgin grades, showing how the linear trend of Fig. 2 found for the virgin grades is also confirmed in case the components are blended together. Thus, according to these findings, the melting peak temperature of PE represents a reliable parameter to identify the type of PE present in the real recycled grades.

Fig. 4 shows how the standard DSC measurement is not able to differentiate the LDPE and HDPE components within the PE fraction of the model blends prepared, as they appear almost completely overlapped, except for one blend with 20 wt% LDPE, where LDPE contribution to the melting appears slightly visible as a peak shoulder (Fig. 4, purple curve). With the aim of attempting a differentiation of the components of the PE fraction, the TM-DSC analysis was applied to all model blends prepared in this work.

The NR-HF scan was analyzed for all model blends prepared in this study, and a method was developed for differentiating the LDPE and HDPE contributions to the PE fraction in the recyclates. Given the sometimes very complex shapes of the NR-HF traces, which may introduce large variability to the results based on operator's choice of integration limit, a code was written in Wavemetrics IgorPro software in order to carry on exactly the same procedure all the times. The code integrates the scans with a curved baseline, as shown in Fig. 9, setting the integration limits between 40 °C and 180 °C (Fig. 9). Moreover, the peak area, here referred to as Non-Reversing Enthalpy (NR-E), was calculated up to 113 °C, as within this temperature range thermal phenomena are likely related to crystal reorganization/recrystallization occurring in the LDPE fraction [42]. Thus, the NR-E up to 113 °C was obtained for all model PO blends, and it was then correlated to their amount of LDPE, with the aim of obtaining a calibration curve to be used for determining the LDPE fraction in the real recyclates. To the best of our knowledge, the use TM-DSC Analysis, and specifically NR-HF, to differentiate the components of the PE fraction in either model blends or recyclates, has not yet been reported in the literature.

Fig. 10 contains the NR-HF traces of the model PO blend (T)LDPE-920/HDPE-946/PP-H with different compositions (a = 5/45/50, b = 10/40/50 and c = 20/30/50), along with the scans of the neat components: (T)LDPE-920 (light blue curve), HDPE-946 (blue curve). The curves shown here do not display the PP-H peak, as this analysis focuses on the PE fraction. The complete NR-HF and R–HF scans can be found in Fig. S4 and Fig. S5 of the SI. Additionally, in Fig. S6 of SI a magnification of the NR-HF traces of just the three different compositions of the model blend is reported, in order to better observe the thermal behavior of the single components. Two contributions to the NR-HF can be identified for all three blend compositions in Fig. 10 and Fig. S6 (SI): a particularly broad exotherm in the same temperature range as the one measured for the neat (T)LDPE-920 (Fig. 10, light blue curve) and an endothermic contribution around ca. 128 °C, to be attributed to the HDPE-946 fraction.

The contributions of the two PE components appear far more clear here in the NR-HF traces than in the DSC standard ones, as it can be better appreciated by comparing Fig. S2 and Fig. S6 of SI, suggesting the TM-DSC as more suitable for quantitative analysis of the LDPE component within the PE fraction.

Thus, the NR-HF traces were analyzed for all model PO blends and used to develop a calibration curve to determine the LDPE content in recycled POs. As already introduced, the NR-E, calculated up to 113 °C, was correlated to LDPE amount present in all model blends prepared. Results of this correlation are displayed in Fig. 11, showing an overall linear trend obtained for the tested samples. The standard deviation was

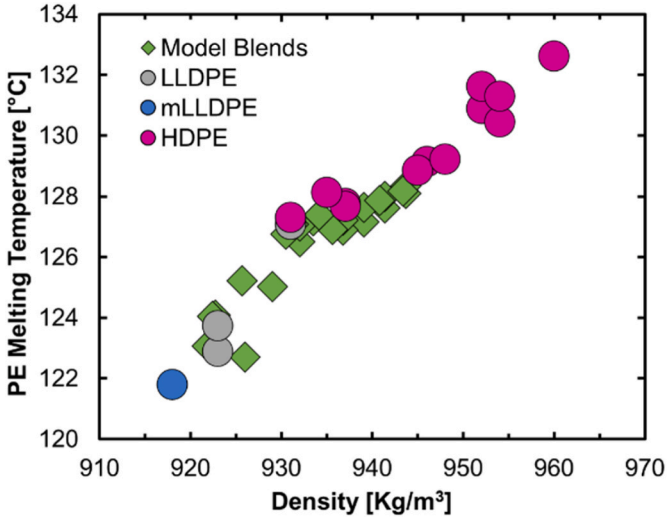

Fig. 8. Peak melting temperature of PE as a function of density, comparison of virgin materials: HDPE (pink dots), (ZN)LLDPE (grey dots), (m)LLDPE (blue dots) and model polyolefin blends prepared (green diamonds). (For interpretation of the references to colour in this figure legend, the reader is referred to the Web version of this article.)

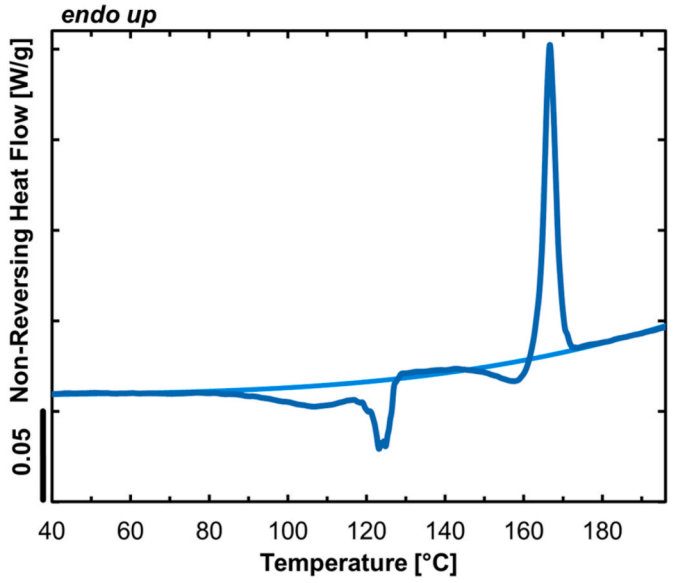

Fig. 9. Schematic of the integration of the NR-HF scan of one of the model blends prepared, integrated by the Wavemetrics IgorPro software with a curved baseline and integration limits 40–180 °C.

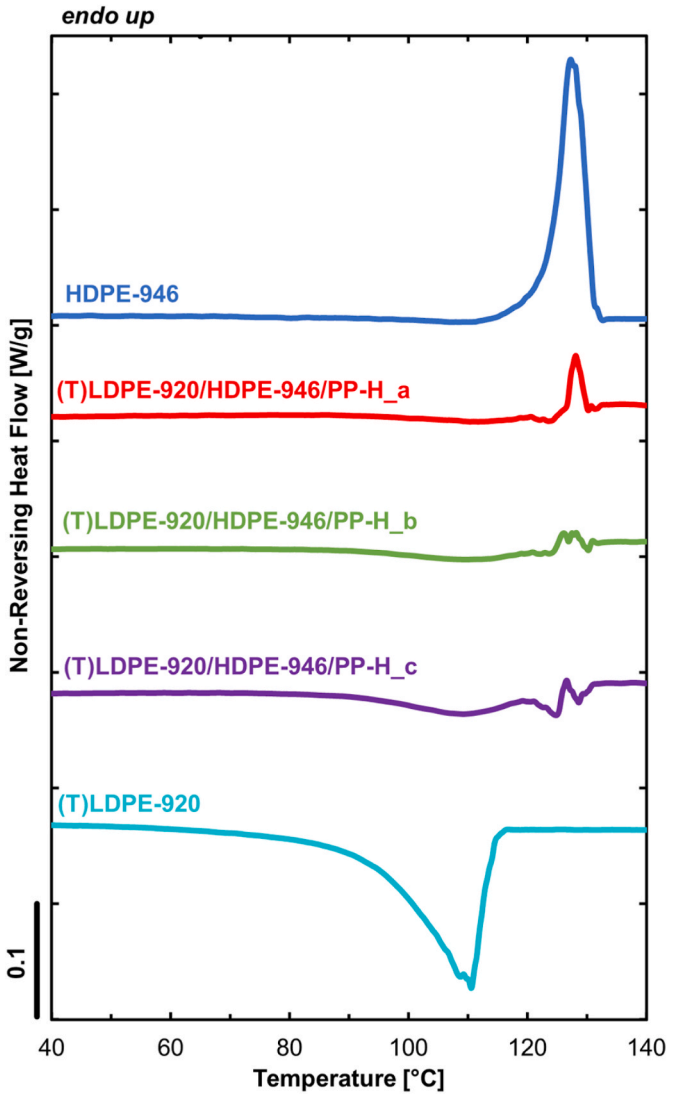

Fig. 10. Non-Reversing heat flow scans of three different compositions of the model PO blend (T)LDPE-920/HDPE-946/PP-H (a = 5/45/50, b = 10/40/50 and c = 20/30/50) along with the ones of the neat PE components used: HDPE-946, (T)LDPE-920.

calculated for the enthalpy values of blends with the same LDPE content, except for the case of blends containing 25 wt%, 50 wt%, and 70 wt% since these were produced only once.

The methods introduced in this work for quantifying PE and LDPE content, based on the TM-DSC analysis of the prepared model PO blends, were applied to two *post*-consumer recycled grades, here indicated as PCR-1 and PCR-2. In detail, these are polyolefin mix recyclates from pre-sorted municipal and household waste. Results from TM-DSC were then compared with the ones obtained from CFC and NMR analysis previously performed on these recycled lots. In detail, 9 TM-DSC measurements were done per each grade, hence average values for the PE and LDPE content have been calculated, as reported in Table 3. Results are here displayed for recyclates that have been homogenized in a micro-compounder, prior to the TM-DSC analysis, to avoid issues related to the representativeness of the low amount of recycled materials analyzed by the technique. Moreover, pellets of PCR-2 have also been measured without previous homogenization, showing different PE and LDPE content together with very large error bars, thus highlighting the importance of this homogenizing step for quantitative analysis. Results from the different techniques showed a good agreement, and the DSC method here introduced proves a valid complement to more well-established analytical techniques.

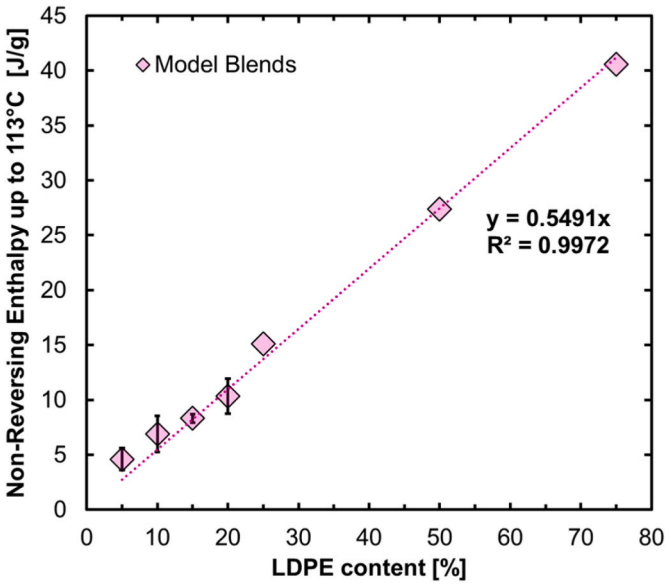

Fig. 11. Non-Reversing enthalpy calculated up to 113 °C as a function of the LDPE content present in the model blends.

Table 3
Results of PE and LDPE content in two post-consumer recycled grades: PCR-1 and PCR-2, obtained from TM-DSC, CFC and NMR. PCR-2 (pellets) refers to a non-homogenized sample.

	DSC	NMR	TM-DSC	CFC
	PE (wt%)	PE (wt%)	LDPE (wt%)	LDPE (wt%)
PCR-1	47.1 ± 0.8	49.5 ± 0.6	15.5 ± 0.9	15.6 ± 1.5
PCR-2	29.1 ± 1.1	26.8 ± 0.6	6.2 ± 0.6	8.1 ± 0.8
PCR-2 (pellets)	25.2 ± 8.5	–	5.2 ± 3.1	–

4. Conclusions

Standard DSC analysis of 29 different virgin PE materials allowed us to find a correlation between the melting temperature (T_m) of each grade and its density. In particular, a linear trend was found for grades with T_m above 120 °C and densities between 918 and 960 kg/m^3. The latter is promising as a calibration curve to predict the density of the PE fraction within the recyclates since direct measurement of this technologically important quantity is not experimentally feasible.

Moreover, the study of the NR-HF traces of the virgin PE materials provided more insights regarding the thermal behavior of the different microstructures tested. PE grades characterized by highly branched structures displayed broad exotherms in all cases, suggesting crystal reorganization phenomena. This feature allows the differentiation of these materials from HDPE grades, for which only endothermic peaks were found in the NR-HF.

Two quantitative methods were developed in order to determine the amount of PE and of the LDPE fraction in the recyclates. As for PE content determination, the second heating scan of a standard DSC analysis of the PE/i-PP model blends was evaluated. Results of the analysis showed a low-temperature tail of the i-PP melting peak overlapping with the melting peak of the PE fraction. Thus, the amount of melting enthalpy of the i-PP phase in the low-temperature range was estimated and subtracted from the overall enthalpy, obtaining the PE content in the blend by calculating the ratio of the corrected enthalpy and the one estimated for a 100% PE material. Results from this method were found to be consistent with the actual PE content in the blends.

Furthermore, by considering the NR-HF traces of the model blends

prepared, a differentiation of the LDPE contribution from the HDPE was obtained. This was achieved by integrating these traces and then establishing a correlation between the NR enthalpy up to 113 °C and the LDPE content in the blends. A linear trend was found to be used as a calibration curve to determine the amount of LDPE within the recyclates. Eventually, the methods were applied to two recycled grades obtained from *post*-consumer waste streams, where results were in agreement with the ones obtained from CFC technique and NMR spectroscopy.

Data availability

The raw data required to reproduce the above findings are available from the authors upon request.

Declaration of competing interest

The authors declare the following financial interests/personal relationships which may be considered as potential competing interests:

Alejandro J. Muller reports financial support was provided by European Union.

Acknowledgements

We acknowledge the financial support from the REPOL project; this project has received funding from the European Union's Horizon 2020 research and innovation program under the Marie Skłodowska-Curie Grant Agreement No. 860221. The authors wish to thank Tamara Carmeli and all the Thermal Analysis group for the help with the TM-DSC measurements, Karin Kemper for the help with procuring the materials, Andreas Albrecht for the CFC measurements, and Gerhard Hubner for the NMR measurements.

Appendix A. Supplementary data

Supplementary data to this article can be found online at https://doi.org/10.1016/j.polymertesting.2022.107656.

References

[1] Plastics Europe - Association of Plastic Manufacturers (Organization), Plastics – the Facts 2020, 2020. https://www.plasticseurope.org/en/resources/market-data.
[2] R. Geyer, Plastic Waste and Recycling, Academic Press, 2020, https://doi.org/10.1016/b978-0-12-817880-5.00014-1.
[3] E.W. Flick, Polyethylenes, Ind. Synth. Resins Handbook, second ed., NOYES PUBLICATIONS, New Jersey, United States of America, 1991 second ed.
[4] M.A. Alma, I. Krupa, Polyolefin Compounds and Materials-Fundamentals and Industrial Applications, Springer, 2016. http://link.springer.com/10.1007/978-3-319-25982-6.
[5] I.A. and O.I. Oluranti A, Rotimi S., Touhami M., Polyolefins and the environment, in: Samuel C. O. Ugbolue (Ed.), Polyolefin Fibres-Structure, Prop. Ind. Appl., second ed., Woodhead Publishing (An imprint of Elsevier), Taunton, MA, United States, 2017: pp. 89–133. https://doi.org/10.1533/9781855734852.536.
[6] D. Gola, P. Kumar Tyagi, A. Arya, N. Chauhan, M. Agarwal, S.K. Singh, S. Gola, The impact of microplastics on marine environment: a review, Environ. Nanotechnol. Monit. Manag. 16 (2021), 100552, https://doi.org/10.1016/j.enmm.2021.100552.
[7] G. Swift, Degradable polymers and plastics in landfill sites, Encycl. Polym. Sci. Technol. (2015) 1–13, https://doi.org/10.1002/0471440264.pst457.pub2.
[8] J.M. Garcia, M.L. Robertson, The future of plastics recycling, Science 358 (2017) 870–872, https://doi.org/10.1126/science.aaq0324, 80.
[9] Z.O.G. Schyns, M.P. Shaver, Mechanical recycling of packaging plastics: a review, Macromol. Rapid Commun. 42 (2021) 1–27, https://doi.org/10.1002/marc.202000415.
[10] O. Drzyzga, A. Prieto, Plastic waste management, a matter for the 'community, Microb. Biotechnol. 12 (2019) 66–68, https://doi.org/10.1111/1751-7915.13328.
[11] S.M. Al-Salem, P. Lettieri, J. Baeyens, Recycling and recovery routes of plastic solid waste (PSW): a review, Waste Manag. 29 (2009) 2625–2643, https://doi.org/10.1016/j.wasman.2009.06.004.
[12] S. Yin, R. Tuladhar, F. Shi, R.A. Shanks, M. Combe, T. Collister, Mechanical reprocessing of polyolefin waste: a review, Polym. Eng. Sci. 55 (2015) 2899–2909, https://doi.org/10.1002/pen.24182.
[13] N. Singh, D. Hui, R. Singh, I.P.S. Ahuja, L. Feo, F. Fraternali, Recycling of plastic solid waste: a state of art review and future applications, Compos. B Eng. 115 (2017) 409–422, https://doi.org/10.1016/j.compositesb.2016.09.013.
[14] M. Roosen, N. Mys, M. Kusenberg, P. Billen, A. Dumoulin, J. Dewulf, K.M. Van Geem, K. Ragaert, S. De Meester, Detailed analysis of the composition of selected plastic packaging waste products and its implications for mechanical and thermochemical recycling, Environ. Sci. Technol. 54 (2020) 13282–13293, https://doi.org/10.1021/acs.est.0c03371.
[15] V. Lahtela, M. Hyvärinen, T. Kärki, Composition of plastic fractions in waste streams: toward more efficient recycling and utilization, Polymers 11 (2019) 1–7, https://doi.org/10.3390/polym11010069.
[16] H. Dahlbo, V. Poliakova, V. Mylläri, O. Sahimaa, R. Anderson, Recycling potential of post-consumer plastic packaging waste in Finland, Waste Manag. 71 (2018) 52–61, https://doi.org/10.1016/j.wasman.2017.10.033.
[17] A. Gala, M. Guerrero, J.M. Serra, Characterization of post-consumer plastic film waste from mixed MSW in Spain: a key point for the successful implementation of sustainable plastic waste management strategies, Waste Manag. 111 (2020) 22–33, https://doi.org/10.1016/j.wasman.2020.05.019.
[18] E. Foschi, F. D'Addato, A. Bonoli, Plastic waste management: a comprehensive analysis of the current status to set up an after-use plastic strategy in Emilia-Romagna Region (Italy), Environ. Sci. Pollut. Res. 28 (2021) 24328–24341, https://doi.org/10.1007/s11356-020-08155-y.
[19] S. Serranti, G. Bonifazi, Techniques for Separation of Plastic Wastes, Elsevier Ltd, 2019, https://doi.org/10.1016/b978-0-08-102676-2.00002-5.
[20] B. Ruj, V. Pandey, P. Jash, V.K. Srivastava, Sorting of plastic waste for effective recycling, Int. J. Appl. Sci. Eng. Res. 4 (2015) 564–571. www.ijaser.com.
[21] P. Rem, F. Di Maio, B. Hu, G. Houzeaux, L. Baltes, M. Tierean, Magnetic fluid equipment for sorting secondary polyolefins from waste, Environ. Eng. Manag. J. 12 (2013) 951–958, https://doi.org/10.30638/eemj.2013.118.
[22] F. Bezati, D. Froelich, V. Massardier, E. Maris, Addition of tracers into the polypropylene in view of automatic sorting of plastic wastes using X-ray fluorescence spectrometry, Waste Manag. 30 (2010) 591–596, https://doi.org/10.1016/j.wasman.2009.11.011.
[23] J.W. Teh, A. Rudin, J.C. Keung, A review of polyethylene–polypropylene blends and their compatibilization, Adv. Polym. Technol. 13 (1994) 1–23, https://doi.org/10.1002/adv.1994.060130101.
[24] R. Shanks, J. Li, L. Yu, Polypropylene–polyethylene blend morphology controlled by time–temperature–miscibility, Polymer 41 (2000) 2133–2139.
[25] C. Aumnate, N. Rudolph, M. Sarmadi, Recycling of polypropylene/polyethylene blends: effect of chain structure on the crystallization behaviors, Polymers 11 (2019), https://doi.org/10.3390/polym11091456.
[26] C. Samuel, T. Parpaite, M.F. Lacrampe, J. Soulestin, O. Lhost, Melt compatibility between polyolefins: evaluation and reliability of interfacial/surface tensions obtained by various techniques, Polym. Test. 78 (2019) 1–29, https://doi.org/10.1016/j.polymertesting.2019.105995.
[27] A. Prasad, A quantitative analysis of low density polyethylene and linear low density polyethylene blends by differential scanning calorimetery and fourier transform infrared spectroscopy methods, Polym. Eng. Sci. 38 (1998) 1716–1728, https://doi.org/10.1002/pen.10342.
[28] J.W. Teh, Structure and properties of polyethylene–polypropylene blend, J. Appl. Polym. Sci. 28 (1983) 605–618, https://doi.org/10.1002/app.1983.070280216.
[29] T. Furukawa, H. Sato, Y. Kita, K. Matsukawa, H. Yamaguchi, S. Ochiai, H. W. Siesler, Y. Ozaki, Molecular structure, crystallinity and morphology of polyethylene/polypropylene blends studied by Raman mapping, scanning electron microscopy, wide angle X-ray diffraction, and differential scanning calorimetry, Polym. J. 38 (2006) 1127–1136, https://doi.org/10.1295/polymj.PJ2006056.
[30] Å.G. Larsen, K. Olafsen, B. Alcock, Determining the PE fraction in recycled PP, Polym. Test. 96 (2021), 107058, https://doi.org/10.1016/j.polymertesting.2021.107058.
[31] M. Gall, P.J. Freudenthaler, J. Fischer, R.W. Lang, Characterization of composition and structure–property relationships of commercial post-consumer polyethylene and polypropylene recyclates, Polymers 13 (2021), https://doi.org/10.3390/polym13101574.
[32] W. Camacho, S. Karlsson, NIR, DSC, and FTlR as quantitative methods for compositional analysis of blends of polymers obtained from recycled mixed plastic waste, Polym. Eng. Sci. 41 (2001) 1626–1635.
[33] R. Juan, B. Paredes, R.A. García-Muñoz, C. Domínguez, Quantification of PP contamination in recycled PE by TREF analysis for improved the quality and circularity of plastics, Polym. Test. 100 (2021), https://doi.org/10.1016/j.polymertesting.2021.107273.
[34] E. Carmeli, D. Tranchida, A. Albrecht, A.J. Müller, D. Cavallo, A tailor-made Successive Self-nucleation and Annealing protocol for the characterization of recycled polyolefin blends, Polymer 203 (2020), 122791, https://doi.org/10.1016/j.polymer.2020.122791.
[35] C. Schick, Differential scanning calorimetry (DSC) of semicrystalline polymers, Anal. Bioanal. Chem. 395 (2009) 1589–1611, https://doi.org/10.1007/s00216-009-3169-y.
[36] L. Raka, G. Bogoeva-Gaceva, Crystallization of polypropylene : application of differential scanning calorimetry, Contrib. Sect. Nat. Math. Biotech. Sci. 29 (2008) 49–67.
[37] A.A. Donatelli, Characterization of multicomponent polyethylene blends by differential scanning calorimetry, J. Appl. Polym. Sci. 23 (1979) 3071–3076, https://doi.org/10.1002/app.1979.070231026.
[38] E. Karaagac, M.P. Jones, T. Koch, V.M. Archodoulaki, Polypropylene contamination in post-consumer polyolefin waste: characterisation, consequences and compatibilisation, Polymers 13 (2021), https://doi.org/10.3390/polym13162618.

[39] A. Manivannan, M.S. Seehra, Identification and quantification of polymers in waste plastics using differential scanning calorimetry, ACS Div. Fuel Chem. Prepr. 42 (1997) 1028–1030.
[40] C. Liu, J. Wang, J. He, Rheological and thermal properties of m-LLDPE blends with m-HDPE and LDPE, Polymer 43 (2002) 3811–3818, https://doi.org/10.1016/S0032-3861(02)00201-X.
[41] E. Verdonck, K. Schaap, L.C. Thomas, A discussion of the principles and applications of Modulated Temperature DSC (MTDSC), Int. J. Pharm. 192 (1999) 3–20, https://doi.org/10.1016/S0378-5173(99)00267-7.
[42] J. Chau, I. Garlicka, C. Wolf, J. Teh, Modulated DSC as a tool for polyethylene structure characterization, J. Therm. Anal. Calorim. 90 (2007) 713–719, https://doi.org/10.1007/s10973-007-8527-4.
[43] M. Reading, D.J. Hourston, in: Modulated-Temperature Differential Scanning Calorimetry: Theoretical and Practical Applications in Polymer Characterisation, Springer, 2006.
[44] M. Reading, A. Luget, R. Wilson, Modulated differential scanning calorimetry, Thermochim. Acta 238 (1994) 295–307, https://doi.org/10.1016/S0040-6031(94)85215-4.
[45] B. Wunderlich, Y. Jin, A. Boller, Mathematical description of DSC based on periodic temperature modulation, Thermochim. Acta 238 (1994) 277–293.
[46] K.J. Jones, I. Kinshott, M. Reading, A.A. Lacey, C. Nikolopoulos, H.M. Pollock, The origin and interpretation of the signals of MTDSC, Thermochim. Acta (1997) 187–199, https://doi.org/10.1016/s0040-6031(97)00096-8, 304–305.
[47] B.B. Sauer, W.G. Kampert, E. Neal Blanchard, S.A. Threefoot, B.S. Hsiao, Temperature modulated DSC studies of melting and recrystallization in polymers exhibiting multiple endotherms, Polymer 41 (2000) 1099–1108, https://doi.org/10.1016/S0032-3861(99)00258-X.
[48] B. Wunderlich, I. Okazaki, K. Ishikiriyama, A. Boller, Melting by temperature-modulated calorimetry, Thermochim. Acta 324 (1998) 77–85, https://doi.org/10.1016/s0040-6031(98)00525-5.
[49] B. Wunderlich, Reversible crystallization and the rigid-amorphous phase in semicrystalline macromolecules, Prog. Polym. Sci. 28 (2003) 383–450, https://doi.org/10.1016/S0079-6700(02)00085-0.
[50] F. Cser, J. H, E. K, Reversible melting of semi-crystalline polymers, J. Therm. Anal. 53 (1998) 493–508.
[51] F. Cser, R.A. Shanks, Annealing of polypropylene polyethylene blends near to the melting points in TMDSC, J. Therm. Anal. 54 (1998) 637–650.
[52] F. Cser, J. Hopewell, E. Kosior, Reversible melting of semicrystalline polymers 2. Annealing near to the melting point, J. Therm. Anal. 53 (1998) 493–508.
[53] G. Amarasinghe, F. Chen, A. Genovese, R.A. Shanks, Thermal memory of polyethylenes analyzed by temperature modulated differential scanning calorimetry, J. Appl. Polym. Sci. 90 (2003) 681–692, https://doi.org/10.1002/app.12694.
[54] R. Androsch, B. Wunderlich, Analysis of the degree of reversibility of crystallization and melting in poly(ethylene-co-1-octene), Macromolecules 33 (2000) 9076–9089, https://doi.org/10.1021/ma000504h.
[55] J. Pak, B. Wunderlich, Melting and crystallization of polyethylene of different molar mass by calorimetry, Macromolecules 34 (2001) 4492–4503, https://doi.org/10.1021/ma010195a.
[56] G.W.H. Höhne, L. Kurelec, S. Rastogi, P.J. Lemstra, Temperature-modulated differential scanning calorimetric measurements on nascent ultrahigh molecular mass polyethylene, Thermochim. Acta 396 (2003) 97–108, https://doi.org/10.1016/S0040-6031(02)00528-2.
[57] G. Amarasinghe, R.A. Shanks, TMDSC analysis of single-site copolymer blends after thermal fractionation, J. Therm. Anal. Calorim. 78 (2004) 349–361, https://doi.org/10.1023/B:JTAN.0000042181.39589.e8.
[58] A. Shamiri, M.H. Chakrabarti, S. Jahan, M.A. Hussain, W. Kaminsky, P.V. Aravind, W.A. Yehye, The influence of Ziegler-Natta and metallocene catalysts on polyolefin structure, properties, and processing ability, Materials 7 (2014) 5069–5108, https://doi.org/10.3390/ma7075069.
[59] M. Zhang, D.T. Lynch, S.E. Wanke, Characterization of commercial linear low-density polyethylene by TREF-DSC and TREF-SEC cross-fractionation, J. Appl. Polym. Sci. 75 (2000) 960–967, https://doi.org/10.1002/(SICI)1097-4628(20000214)75:7<960::AID-APP13>3.0.CO;2-R.
[60] J.D. Hoffman, Treatise on Solid State Chemistry, Volume 3 – Crystalline and noncrystalline solids, in: Plenum Press, New York, 1976: p. 774 pp.
[61] W.F. Msuya, C.Y. Yue, The correlation between the lamellar thickness and the degree of crystallinity in semicrystalline polymers, J. Mater. Sci. Lett. 8 (1989) 1266–1268, https://doi.org/10.1007/BF00721488.
[62] A. Włochowicz, M. Eder, Distribution of lamella thicknesses in isothermally crystallized polypropylene and polyethylene by differential scanning calorimetry, Polymer 25 (1984) 1268–1270, https://doi.org/10.1016/0032-3861(84)90374-4.
[63] V.B.F. Mathot, R.L. Scherrenberg, T.F.J. Pijpers, Metastability and order in linear, branched and copolymerized polyethylenes, Polymer 39 (1998) 4541–4559, https://doi.org/10.1016/S0032-3861(97)10306-8.
[64] S. Hosoda, K. Kojima, M. Furuta, Morphological study of melt-crystallized linear low-density polyethylene by transmission electron microscopy, Makromol. Chem. 187 (1986) 1501–1514, https://doi.org/10.1002/macp.1986.021870619.
[65] S. Jose, A.S. Aprem, B. Francis, M.C. Chandy, P. Werner, V. Alstaedt, S. Thomas, Phase morphology, crystallisation behaviour and mechanical properties of isotactic polypropylene/high density polyethylene blends, Eur. Polym. J. 40 (2004) 2105–2115, https://doi.org/10.1016/j.eurpolymj.2004.02.026.
[66] E. Carmeli, G. Kandioller, M. Gahleitner, A.J. Müller, D. Tranchida, D. Cavallo, Continuous cooling curve diagrams of isotactic-polypropylene/polyethylene blends: mutual nucleating effects under fast cooling conditions, Macromolecules 54 (2021) 4834–4846, https://doi.org/10.1021/acs.macromol.1c00699.
[67] B.J. Luijsterburg, Mechanical Recycling of Packaging Waste, Technische Universiteit Eindhoven, 2015, https://doi.org/10.1016/b978-0-12-817880-5.00011-6.
[68] S. Hubo, L. Delva, N. Van Damme, K. Ragaert, Blending of recycled mixed polyolefins with recycled polypropylene: effect on physical and mechanical properties, AIP Conf. Proc. 1779 (2016), https://doi.org/10.1063/1.4965586.
[69] L. Delva, L. Cardon, K. Ragaert, Evaluation of post-consumer mixed polyolefines and their injection moulded blends with virgin polyethylene, Environ. Eng. Manag. J. 17 (2018) 427–434, https://doi.org/10.30638/eemj.2018.043.